Thriving Through Climate Change and Pandemic Symposium
Windsor, Ontario, Canada
June 24-25, 2021

Studying the Influential Parameters in an Office Building's Energy Consumption

Naveen R.K.S. Bhoopal, Jacqueline A. Stagner*, David S-K. Ting
Turbulence and Energy Laboratory, University of Windsor
401 Sunset Ave, Windsor, ON, Canada

Abstract

Research on the energy consumption of buildings has become increasingly important due to the growing global population and depleting energy resources. This study focuses on modeling the energy usage of an office building by examining the various parameters that influence its electricity consumption. An existing office building located in Philadelphia is selected as a reference for simulation, and the simulated results and measured values are compared. The parameters that affect the building, such as ambient temperature, solar radiation, building envelope, wind speed, and other internal gains, are discussed and defined. To verify the model, a transient simulation is run for sinusoidal ambient weather data for 180 hours, with a timestep of 15 minutes. The thermal mass and thermal resistance of the building envelope cause the expected delay and attenuation in the indoor temperature and indoor power demand. The building is then subjected to real case inputs from the actual office building for predictive modeling. The simulation output is compared with the measured power consumption data from the literature, which is provided for each month over the course of a full year (2004). To account for the variability of a building's infiltration rate over a year, the results are plotted for two different infiltration values: 0.25 ACH and 0.85 ACH. It is found that the simulated results for the two infiltration values provided are within the range of the measured values. This study provides valuable information on the factors that affect the energy usage of office buildings. The simulation results demonstrate the predictability of modeling an office building energy usage. As part of future work, this model will be employed to perform a sensitivity analysis on energy consumption for each parameter, with the aim of pinpointing the parameter that exerts the most substantial influence.

1. Introduction

Buildings consume approximately 40% of global energy [1]. This proportion is expected to increase globally with population growth in the next 20 years [2]. In the United States, commercial buildings are responsible for the majority of energy usage per square meter, consuming approximately 1995 GWh of total energy in 2018 [3]. Among the various types of commercial buildings, office buildings are the most energy-intensive, consuming roughly 300 GWh in total, with electricity accounting for 75% and natural gas for the remaining 25% [4]. In Figure 1, the energy consumption data for various commercial building types in 2018 is depicted, revealing that office buildings exhibit the most substantial energy usage. Therefore, it is essential to discuss the intricacies of energy consumption in office buildings, as they play a significant role in overall energy usage and have considerable potential for energy savings.

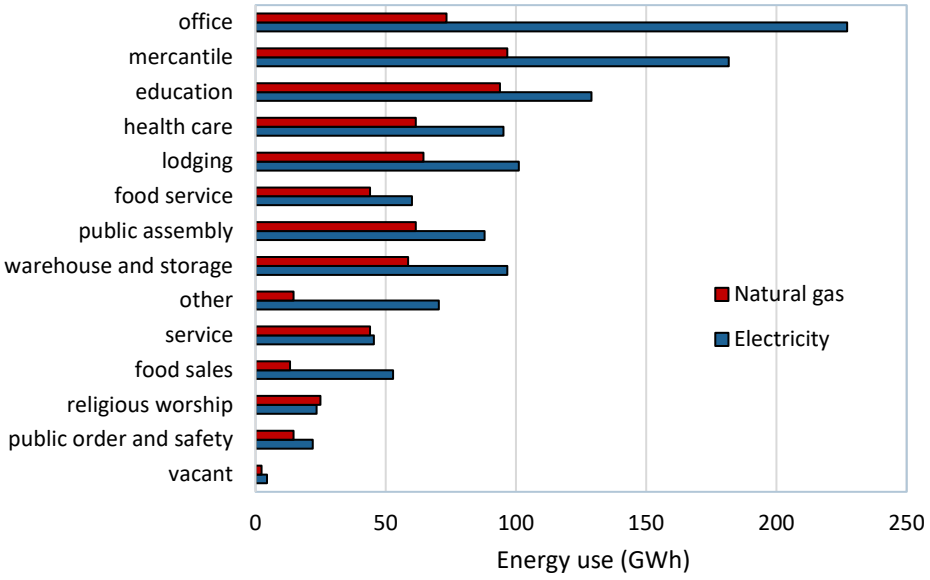

*Corresponding author
Email address: stagner@uwindsor.ca (J. A. Stagner)

Fig 1. Types of commercial buildings and their energy usage in the US in 2018, based on [4].

The energy consumption of a building is shaped by various parameters, but certain ones hold particular significance and necessitate dedicated scrutiny. These can be categorized into environmental parameters and building parameters. The former involves ambient temperature, solar radiation, ground temperature, and heat transfer coefficient, while the latter encompasses lighting, equipment, HVAC units, occupancy, windows, and walls (as illustrated in Fig. 2).

The power load of a building is significantly affected by environmental factors, which cannot be controlled. Among these factors, ambient temperature has a particularly noteworthy impact on building energy consumption, and this impact has been exacerbated by climate change [5,6]. Papakostas et al. [6] explored changes to heating and cooling loads in Athens resulting from rising ambient temperatures over the past decade, which they attributed to climate change. According to their model, the heating load is projected to decrease by 14%, while the cooling load is estimated to increase by 44%.

Following ambient temperature, the contribution of solar radiation is highly notable [7,8]. The solar radiation is incident on the building in the form of three components: beam radiation, diffuse radiation, and ground reflected radiation. Huang and Liu [9] found that solar radiation contributes to 26.12% of energy consumption during the winter season for a building in Western Sichuan. The incident radiation on the windows of the building is transmitted, absorbed, and reflected, while on opaque walls, it is only absorbed and reflected.

Another critical parameter that significantly impacts a building's energy consumption is the building envelope. The amount of solar heat gain entering the building is determined by the thermal properties of the windows and opaque walls, which include transmissivity, solar absorptance, and window-to-wall ratio (WWR). For example, according to ASHRAE standard 90.1, commercial buildings should have a maximum of 40% WWR in the United States to minimize energy use.

Furthermore, infiltration and exfiltration are the air entering and exiting (respectively) the building through the leaks and cracks of the building envelope. Infiltration accounts for approximately 15% to 30% of total energy consumption (heating and cooling loads) in office buildings in the United States [10,11]. The unit of measure is called the air infiltration rate (α, h^{-1}), which depends on the airflow rate (Q, m^3/s) and volume of the indoor space unit (V_i, m^3) by:

$$\alpha = \frac{Q}{3600 V_i} \quad , \tag{1}$$

where the airflow rate is given by [12]:

$$Q = \frac{A_{ELA} C_D}{10000} \sqrt{\frac{2\Delta P}{\rho}} \quad , \tag{2}$$

and C_D is the air discharge coefficient, A_{ELA} is the air leakage area on the wall surface (m^2), ΔP is the pressure difference due to wind speed (Pa), and ρ is the density of air (kg/m^3). In addition, ventilation rate, expressed as the amount of air entering or leaving a building, is measured in air changes per hour (ACH), the same unit used for infiltration rate. Ventilation in office buildings can be divided into two main categories: natural ventilation and mechanical ventilation [13]. According to ANSI/ASHRAE standard 62.1-2022, Ventilation and Acceptable Indoor Air Quality [14], the ventilation air flow rate for office spaces is given as 0.06 cfm/sf, which can be converted to 1.098 $m^3/hr/m^2$ in SI units. This can be converted to ACH (h^{-1}) by multiplying the floor surface area and dividing it by the volume of the room.

Internal heat gains are a significant contributor to a building's energy consumption, which largely originate from sources such as lighting, equipment, and occupancy. Lighting has been found to be the most significant contributor to overall energy consumption, accounting for 20% to 40% of energy usage [15-17]. Recent studies suggest the preferred lighting density for an office workspace is from 13.4 W/m^2 to 16.7 W/m^2 [18]. Likewise, the equipment load density for office buildings typically falls within a range of 10 W/m^2 to 18 W/m^2 [19]. In the case of occupancy, it changes with building space, as the allowance is given in terms of number of people per foot exit from egress building code.

Finally, the ground is a parameter which acts as a heat sink during summer and a heat source during winter. The earth is solid ground that is of infinite thickness when compared to the size of the building. Therefore, the heat transfer between the ground and the building is different from other common heat transfer modes (conduction, etc.). Several equation models have been developed to calculate the ground temperature according to various parameters like depth,

ambient temperature, etc., in aiming to obtain accurate results when compared to measured values [20-22]. In this paper, TRNSYS software is used, which uses one such ground model to calculate the ground temperatures. This is discussed in detail in section 2.2.1. TRNSYS is commonly used to calibrate energy data in transient analyses with a defined time step, and its applicability to building energy simulations for structures of varying complexity has been demonstrated [23]. The software proves to be user-friendly for energy simulations and has significant advantages over other simulation software. This paper confirms the reliability of TRNSYS for subsequent simulations of the same building model, by exploring the thermal mass of the building envelope.

This study develops a predictive model for an office building's energy consumption. Although there has been much research on energy consumption prediction, it is still challenging to predict energy usage with any degree of accuracy without providing thorough justification and details [24-26]. This study addresses this limitation by simulating a range of building energy consumption values to consider the real-life challenges that affect the accuracy of the prediction.

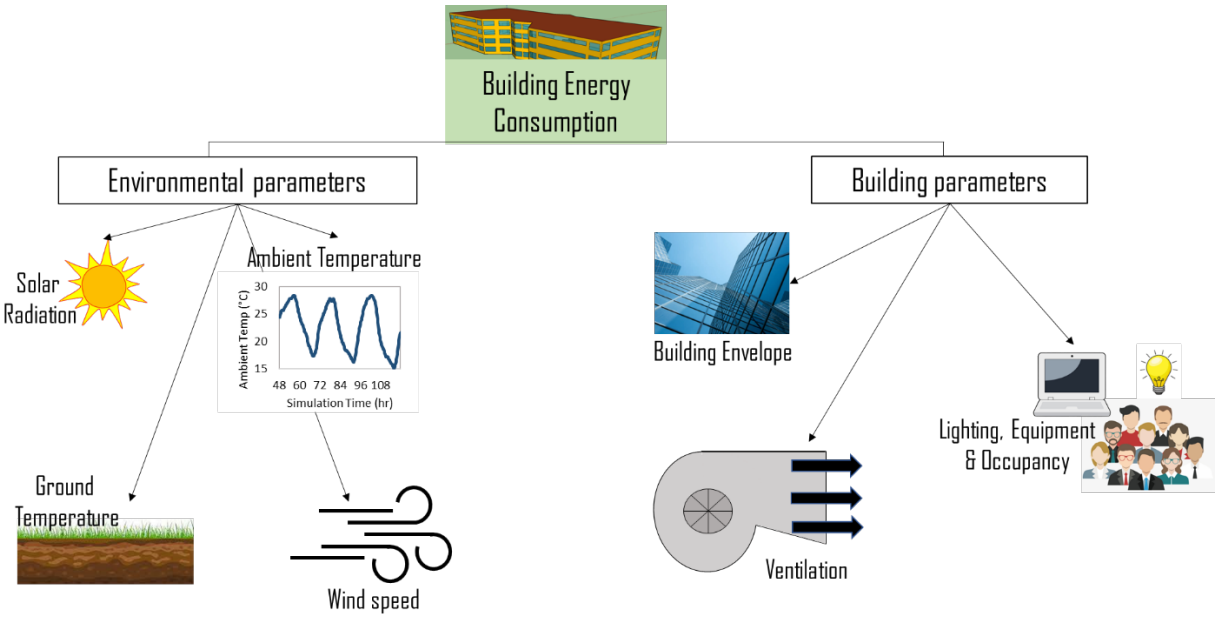

Fig 2. Influential parameters for a building's energy consumption

2. Methodology

SketchUp software is used to create a model of an existing building from the information provided in Reddy et al. [27-29]. To study the impact of environmental and building parameters, data for each month was analyzed separately. Hourly dry bulb temperature data is extracted from National Solar Radiation Database (NSRDB) for the year 2004 as the available temperature data model in TRNSYS is for a typical meteorological year (TMY). However, TMY data was utilized for solar radiation due to the complexity of the parameters involved. The model is imported as a multi-zone building in TRNSYS using the trnsys3d addon in SketchUp software. The following parameters or building inputs are defined in TRNBuild and are discussed below: building envelope material, workday schedule, infiltration, ventilation, heating input, cooling input, and internal gains like lighting, equipment, and occupancy.

2.1 Preprocessing

2.1.1 *Building case study*

The office building selected for this study is located at 400 Campus Drive, Collegeville, Philadelphia. It is a four-storey building with a floor area of 2500 m^2. The vertical wall is constructed with concrete masonry units (CMU) with concrete between hollow blocks, as shown in Fig. 3 [30]. The roof is fabricated with concrete and a layer of insulation, while the floors are made of lightweight concrete (Fig. 3). Table 1 contains information on the conductivity values, wall thickness, and heat capacity of the building envelope. The list of material property values is extracted from Reddy

et al. [27-29], while the values marked with an asterisk are obtained from the TRNSYS library. The values in TRNSYS library are derived from trusted sources like ASHRAE fundamentals and German sources like SIA 2024, VDI 2078.

A front view and top view of the office building is shown in Fig. 4(a). The building's exterior vertical walls are painted red with a solar absorptance of 0.6, while the roof is painted white with a solar absorptance of 0.4. The orientation of the building is 5° west of north as shown in Fig 4(b). Double-glazed windows are installed in the building with a window-to-wall ratio (WWR) of 0.4 and with u-value, g-value, and transmissivity given as 2.78 W/m^{2}K, 0.59, and 0.61, respectively [27-29]. They are encased in a hardwood frame with a 0.15 window-frame fraction.

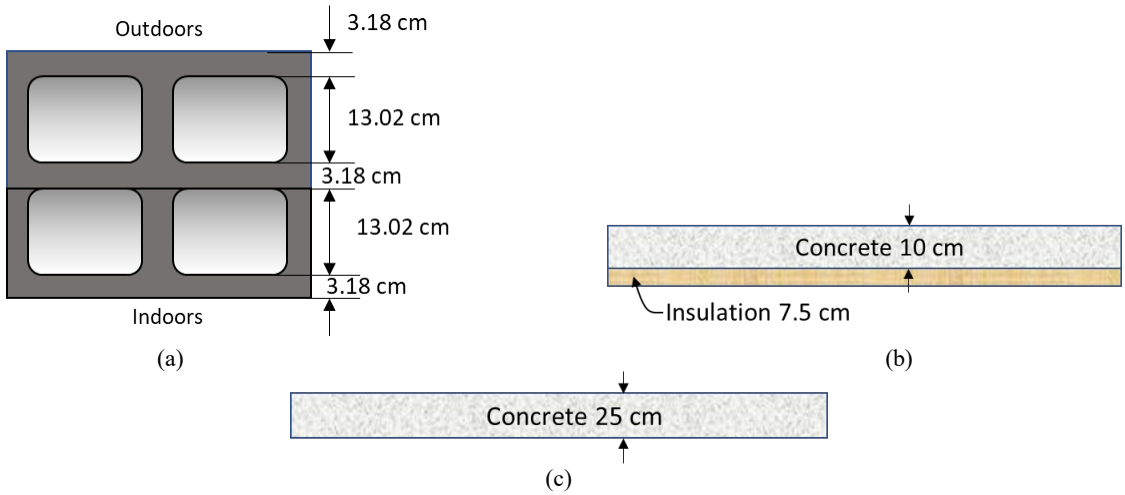

Fig 3. Building envelope details of (a) vertical walls, (b) Roof and (c) ground floor.

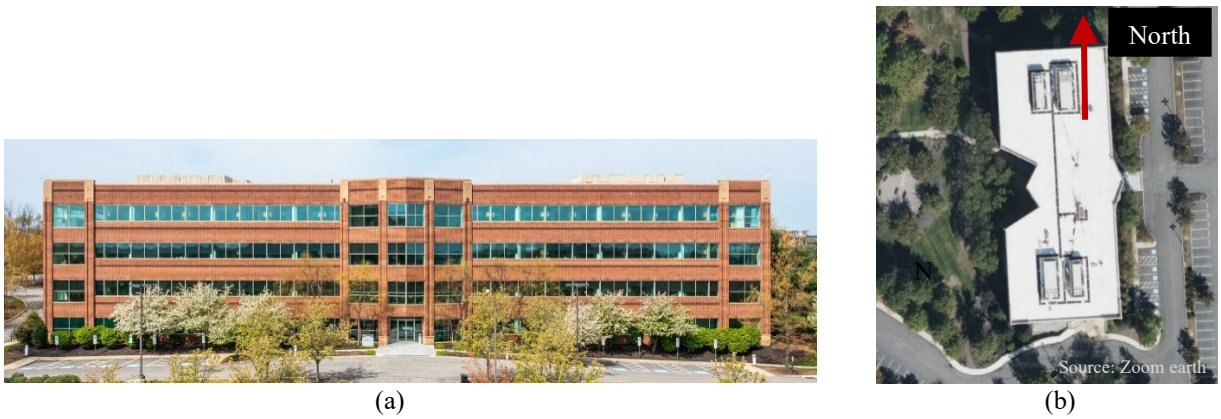

Fig 4. (a) Front view and (b) top view of the office building in Philadelphia.

Table 1. Thermal properties of the building envelope

Properties	**Vertical walls**	**Roof**		**Floor**
	CMU	**Concrete slab**	**Insulation**	**L.W. Concrete**
Conductivity, k (W/m·K)	0.51	4.07	0.11*	1.76*
Heat Capacity, c (kJ/kg·K)	1.00	1.00	1.00	1.00
U-value (W/m^2·K)	0.38	0.37		0.77
Thickness (m)	0.35	0.10	0.075	0.25

*Values obtained from TRNSYS library

2.1.2 SketchUp modeling

Great care was taken in modeling the building to ensure that even minor variations in measurements are reflected in energy usage calculations. To this end, SketchUp was employed as a modeling and simulation tool, with the trnsys3d add-on used to save the model in a compatible format for import into TRNSYS Simulation Studio [31]. Each surface of the building was modeled and classified as either an external wall, roof, ground floor, adjacent floor, adjacent ceiling, or window, as shown in Figure 5.

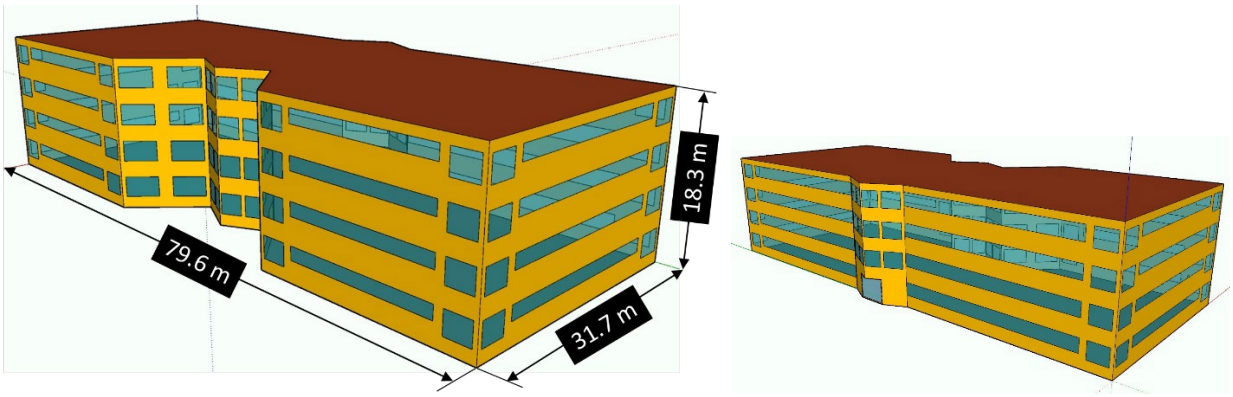

Fig 5. Isometric views of the SketchUp building model

2.2 TRNSYS simulation

The building model in SketchUp is imported in an idf file format to TRNSYS Simulation Studio. Fig. 6 illustrates the Simulation Studio layout in TRNSYS with each icon representing a type-file. The main type-file among the three solar radiation components is the Type 15 file, also called a weather data file. The main parameters involved in the calculation of this file are solar zenith angle, solar azimuth angle, angle of incidence for all surfaces, and beam and diffuse radiation of all surfaces. Secondly, there is the ambient temperature file (Type 9), which accepts the NSRDB dry bulb temperature data in the form of a text file. The ground temperature model is Type 77. These files contain parameters that act as inputs to the Type 56 building model for running the simulation. Finally, the Type 65 file is used to generate the required plots and the results are printed using the Type 25 file. TRNBuild is used to define other modeling parameters of the building like workday schedule, internal gains, outputs needed, heating and cooling, infiltration and ventilation rates, and building envelope information including windows and heat transfer coefficient.

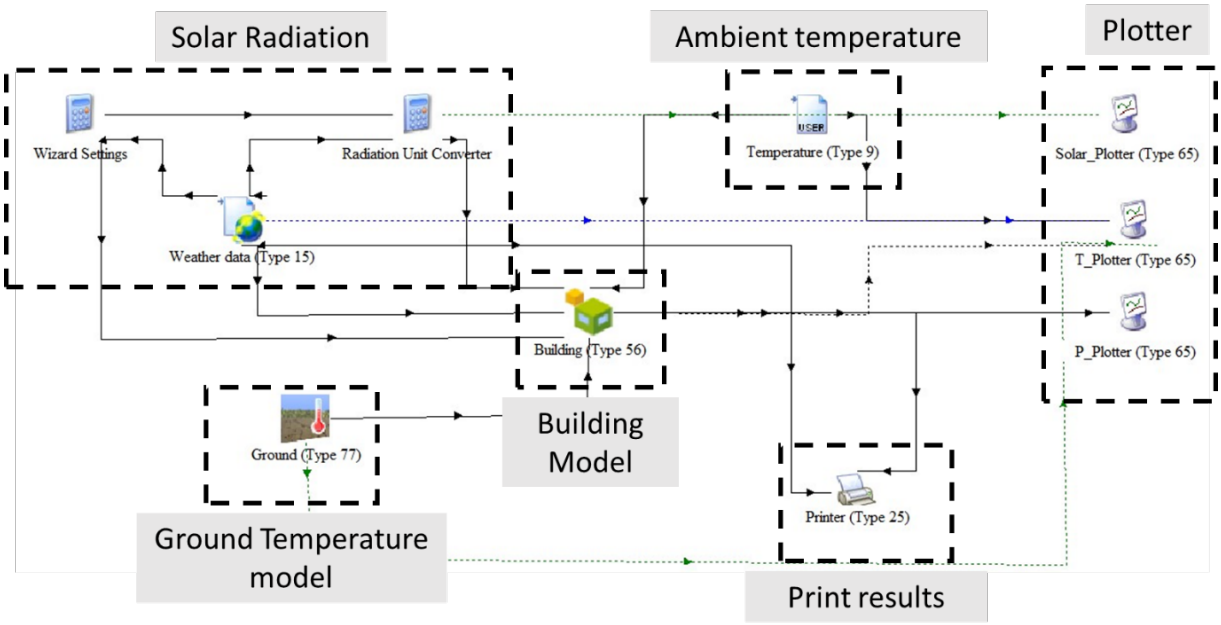

Fig 6. TRNSYS layout of type files in Simulation Studio.

2.2.1 Ground temperature

Unlike other surfaces, the ground floor is directly connected to the earth, which is considered to be solid ground with infinite thickness. TRNSYS uses the concept of Kasuda's Underground Temperature (UGT) model to define the heat transfer between the ground and the building [22],

$$T_G = T_{mean-} - T_{amp} e^{-D\left(\frac{\pi}{365\alpha}\right)^{0.5}} \cos\left(\frac{2\pi}{365}\left(t_{now} - t_{shift} - \frac{D}{2}\left(\frac{365}{\pi\alpha}\right)^{0.5}\right)\right) \quad , \tag{3}$$

where, T_G is the ground temperature (ºC), T_{mean} is the average ambient temperature (ºC), T_{amp} is the amplitude of the surface temperature (ºC), D is the depth below surface (m), α is the thermal diffusivity of the ground (m^2/day), t_{now} is the current day of the year (day), and t_{shift} is the day of the year corresponding to the minimum surface temperature (day). From Equation 2, it can be inferred that ground temperature varies with ambient temperature, depth, and thermal properties of the ground. The important thing to observe is the understanding of heat transfer between the ground and the building. Two main points can be noted here: (1) the building is attached directly to the earth/ground, and (2) ground temperature varies with depth. The outer surface of the ground floor has a temperature that varies according to Equation 2 with D=0. Now, this can be considered a standard heat transfer problem with conduction through the ground floor and convection to the indoors.

2.2.2 Heat transfer around the building

The incident solar radiation from the sun and the convective heat gain from the temperature difference between indoor and outdoor are the main contributors in the heat balance equation. This heat is transferred to the indoors by conduction through opaque walls, given by the following equation (all units are in W/m^2):

$$q_{cond} = q_{SW} + q_{conv} + q_{LW} \quad , \tag{4}$$

where q_{cond} is the heat flux through conduction, q_{SW} is the shortwave radiation, q_{LW} is the longwave radiation, and q_{conv} is the convective heat flux. The convective heat transfer coefficient exhibits variability with wind speed leading to discernable differences between indoors and outdoors of the building. The TRNSYS default value for the convective heat transfer coefficient inside a building is h_i = 3 W/m^2·K. In outdoor environments, wind speed can fluctuate significantly throughout the year. Strong winds that encourage heat exchange between the building and the surrounding air during winter often result in a greater convective heat transfer coefficient. In contrast, the convective heat transfer coefficient is significantly lower in the summer since there are fewer opportunities for heat transfer due to slower winds [32]. The relation between the wind speed and convective heat transfer coefficient is given by the following equation obtained from regression analysis for the central area of the building in outdoor conditions [33]:

$$h = 1.444v + 4.955 \quad , \tag{5}$$

where v is the wind speed and h is the convective heat transfer coefficient. However, since the wind speed impact is greater on the edges of the building compared to central area, Sparrow and Ramsey [34] found the average heat transfer coefficient is 1.18 times the central area heat transfer coefficient,

$$h_{av} = 1.18\, h \;=\; 1.7v \;+\; 5.85\,. \tag{6}$$

Heat transfer coefficient values for vertical and horizontal walls are assumed to vary by the same equation, as a negligible difference has been reported for outdoor conditions [33]. The convective heat transfer coefficient is evaluated for all the months for a year according to the wind speeds in Philadelphia given by Fig. 7 [35].

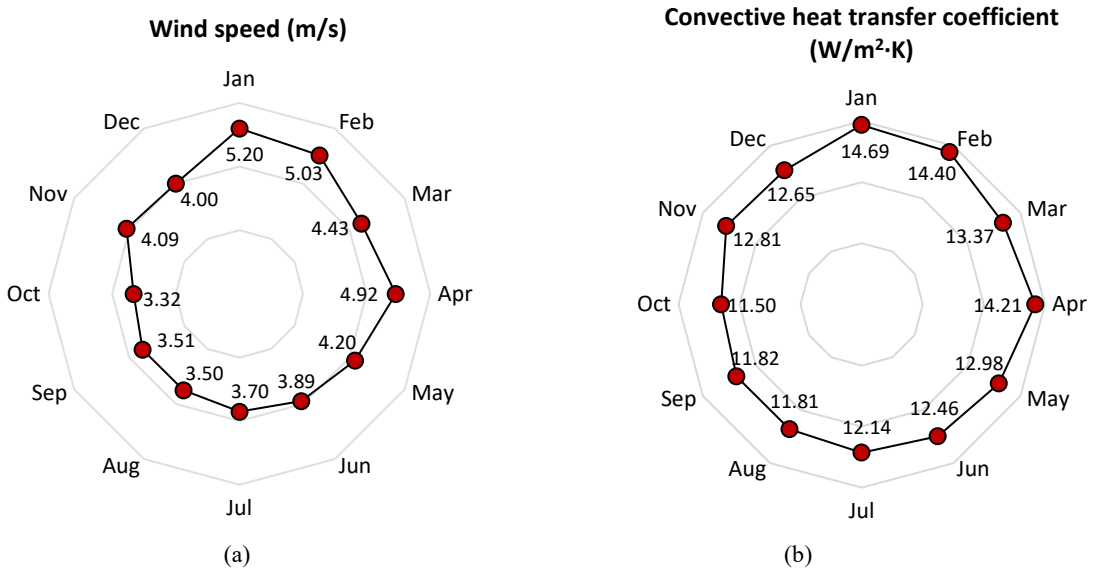

(a) (b)

Fig 7. Monthly average (a) wind speed taken from [35] and corresponding (b) heat transfer coefficient values.

Solar radiation incident on the wall is in the form of three components: beam incident radiation, diffuse incident radiation, and ground reflecting radiation. The total incident radiation is the summation of these three incident radiation components, separated by terms as shown in the following equation [36]:

$$G_t = R_B\, G_B + G_D \left[\frac{1+cos\,\beta}{2}\right] + (G_B + G_D)\rho_G \left[\frac{1-cos\beta}{2}\right] \quad , \tag{7}$$

where R_B is the radiation tilt factor, G_B is the beam radiation for a horizontal surface, G_D is the diffuse radiation for a horizontal surface, β is the tilt angle, and ρ_G is the ground albedo. The building's exterior is exposed to incident radiation on 11 surfaces, excluding the ground level. The solar absorptance values of concrete, and red and white painted walls are 0.6, 0.6, and 0.4, respectively [37]. Consequently, the vertical walls have an overall solar absorptance of 0.36 (0.6 × 0.6), signifying that they absorb 36% of the radiation. Similarly, the roof has an overall solar absorptance of 0.24 (0.6 × 0.4). It is crucial to note that sunlight enters the building through the installed windows on these surfaces. The window-to-wall ratio (WWR) is 0.4, indicating that a maximum of 40% of the total incident radiation on the walls is converted into indoor solar heat gain.

2.2.3 Indoor regime types

The regime types are input information that represent infiltration gain, HVAC systems, and internal gains inside the building. HVAC systems are used to create a comfortable human environment by inducing ventilation and air circulation inside the building [38]. The list of HVAC inputs for the current case includes heating, cooling, ventilation, and the internal gains: lighting, infiltration, equipment density, and occupancy.

2.2.3.1 Infiltration

Air Infiltration in buildings can affect energy consumption and indoor air quality. The infiltration in the buildings is caused by the leaks and cracks present in the building envelope. However, another major factor that influences the infiltration rate is the outdoor wind speed. The kinetic energy from the wind affects the pressure gradient on the surfaces, which in turn impacts the infiltration rate [39]. Furthermore, because wind speeds vary continuously, the building's infiltration rate is described as a range rather than a set amount. Due to the dynamic nature of wind conditions, assuming a fixed infiltration rate can result in modeling inaccuracies and deviations from actual results.

The typical range of infiltration rates for buildings in North America is given from 500 $cm^3/s \cdot m^2$ to 3000 $cm^3/s \cdot m^2$, according to Chapter 16 of 2017 ASHRAE Fundamentals [37]. For the current office building being studied (surface area = 2588 m^2, volume = 12165 m^3, for each floor), the range of infiltration rates in air changes per hour (ACH) is given by

$$Q_{inf-min}(\text{ACH}) = \frac{500cm^3}{12165m3} \times \frac{(60\times60s)}{s\cdot h} \times \frac{2588.3m^2}{m^2} = 0.38\text{h}^{-1} \quad \text{and} \tag{8}$$

$$Q_{inf-max}(\text{ACH}) = \frac{3000cm^3}{12165m3} \times \frac{(60\times60s)}{s\cdot h} \times \frac{2588.3m^2}{m^2} = 2.30\text{h}^{-1} \tag{9}$$

Although the values are called infiltration rates, they are the total ACH values of the building, i.e., including ventilation rates. Focussing on the infiltration gain calculation in TRNSYS, the infiltration heat gain ($\dot{q}_{infl}$, W) is given by:

$$\dot{q}_{infl} = \dot{m}C_p(T_a - T_i) \tag{10}$$

$$\dot{m} = V \times \rho \times \alpha \tag{11}$$

where C_p is the specific heat of air (J/kg·K); $\dot{m}$ is the mass flow rate (kg/s) of infiltration air given by multiplying the volume (V, m^3), density (ρ, kg/m^3), and infiltration rate (α, h^{-1}); and T_a (°C) and T_i (°C) are the ambient temperature and indoor temperature, respectively.

2.2.3.2 Ventilation

Like infiltration, the simulation input for office building ventilation in TRNSYS is given by air exchange rate (α_v, h^{-1}). In addition, the ventilation heat gain ($\dot{q}_{vent}$, W) is calculated using

$$\dot{q}_{vent} = \dot{m}C_p(T_a - T_i) \tag{12}$$

where C_p is the specific heat of air (J/kg·K), $\dot{m}$ is the mass flow rate of ventilation air (kg/s), and T_a (°C) and T_i (°C) are the ambient temperature and indoor temperature, respectively. The ventilation rate of the selected office building with 256 people is given as 7.08 cfm/person [27-29], which, when converted to ACH (air changes per hour), yields]

$$Ventilation\ rate(\alpha_v) = 7.08\frac{cfm}{person} \times 256people = 3840\frac{ft^3}{min} = \frac{1}{1718412ft^3(Volume)} \times \frac{60min}{h} \approx 0.15h^{-1} \tag{13}$$

2.2.3.3 Lighting, equipment and occupancy

The lighting, equipment, and occupancy heat gain information in TRNSYS are given directly in terms of Watts or Watt/$meter^2$. As a result, simply adding individual heat gains yields the final heat load. The lighting density and equipment density is given by 16.1 W/m^2 and 12.38 W/m^2, respectively. From the Chartered Institution of Building Services Engineers (CIBSE) Guide A: Environmental design [40], the average heat emitted by a person is 75 W/person while sitting, standing, or walking in an office space. Therefore for 256 people in the office building, the occupancy gain for the complete building is given by

$$75\frac{W}{person} \times 256people = 19200W. \tag{14}$$

It is important to note that occupant density is given in terms of absolute gain, while the lighting and equipment gains are related to the reference floor area.

The workday schedule of lighting, equipment, and occupancy is depicted in Figure 8. The vertical axis in the plot depicts the proportion of the given density value for lighting, equipment, and occupancy. In other words, during the workday hours of 8:00 am to 6:00 pm, the lighting, equipment, and occupancy are at 90% of full capacity. While in the off-hours (6:00pm-8:00am), lighting is at 10% of full capacity, equipment is at 40% of full capacity, and occupancy is at 5% of full capacity.

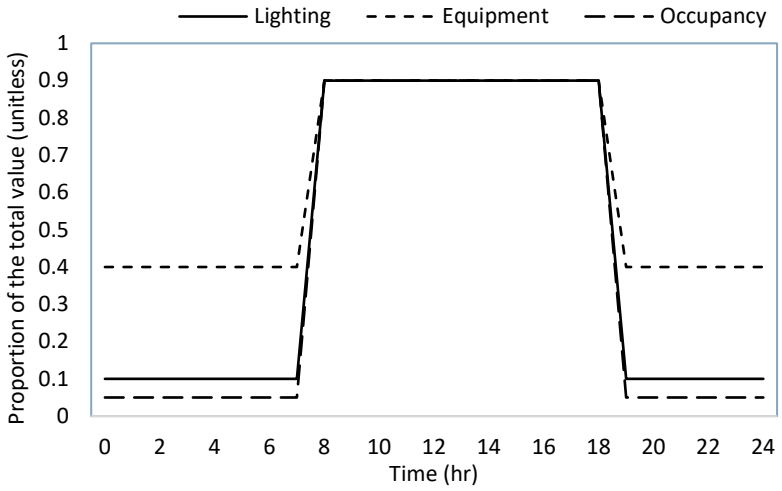

Fig 8. Workday schedule for lighting, equipment, and occupancy

2.2.3.4 Heating and cooling

The temperature settings for heating and cooling are different, to save energy during non-working hours. For instance, the temperature setting for heating during working hours is 23°C, and during non-working hours is 19°C. The temperature setting for cooling during working hours is also 23°C, but during non-working hours is 27°C (Fig. 9). In addition, during the weekends, i.e., Saturday and Sunday, the temperature is set to 19°C for heating and 27°C for cooling. The relative humidity of the building is maintained constant at 50%, according to ASHRAE Standard 55 for occupancy comfort. The total heat balance equation in TRNSYS is given in terms of total power demand (Q_i, W) and is given by

$$Q_i = Q_{infl} + Q_{vent} + Q_{int} + Q_{sol} + Q_{abs} . \quad (15)$$

Here, Q_{infl} is the infiltration gain (Eq. 9); Q_{vent} is the ventilation gain (Eq. 11); Q_{int} is the internal gains like lighting, equipment, and occupancy; Q_{sol} is the fraction of solar radiation through external windows converted to indoor convective gain; and Q_{abs} is the absorbed heat gain on the walls of the building converted to indoor convective gain (all units in W).

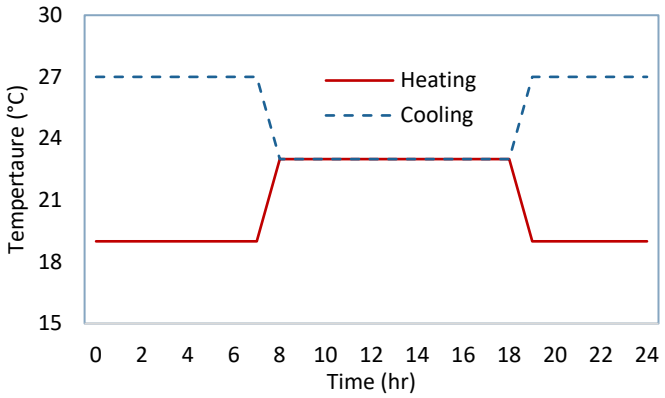

Fig 9. Indoor temperature setting

3. Results and Discussions

As per the usual practice, conducting a computational study requires verification of the software used for modeling. To accomplish this, an analysis is carried out on the indoor temperature and indoor power demand (in kJ/hr) of the building. The purpose of this study is to demonstrate the impact of the thermal mass and thermal resistance of the building envelope on the performance of the model [41]. Through this analysis, the TRNSYS model can be validated for future work. Finally, to model the building, the parameters discussed in the methodology are employed to obtain monthly energy consumption figures, which are compared to the data obtained from Reddy et al. [27-29] to establish the accuracy of the model.

3.1 Verification model

In this case, the behaviour of indoor temperature and indoor power consumption are investigated with ambient temperature as the only input i.e., no effect of solar radiation, infiltration, ventilation, and internal gains on the building. The default time step in TRNSYS is one hour; however, to accommodate for more accuracy, the simulation is carried out with a time step of 15 minutes. Ground temperature is kept at 13°C, which is one degree lower than the mean ambient temperature. A user-defined sinusoidal weather data input is used to study the variation of indoor temperature. The outdoor temperature range values are taken for Philadelphia and are based on the weather reports collected during 1985-2015, to replicate the meteorological data of the real office building [42]. The heating and cooling inputs of the building are turned off to analyse the fluctuation of indoor temperature based on the ambient temperature.

Fig. 10 shows the behavior of indoor temperature (red dashed curve) according to the sinusoidal weather data (blue curve). A delay and attenuation in the indoor temperature is observed in the simulation plot (Fig. 10), because of the finite thermal resistance and finite thermal mass of the building envelope. In other words, not all the heat from the surroundings enters the building due to the building envelope. From the indoor temperature plot (Fig. 10), the following observations are made: (1) due to the ground temperature of 13°C, there is a minor shift in mean indoor temperature by 0.62°C below the mean ambient temperature of 14°C; (2) the indoor temperature has a thermal delay of 15.70 hours when compared to the ambient temperature; and (3) an attenuation value of 9.68°C can be observed in the indoor temperature from the ambient temperature.

Similarly, to check the variation of indoor power demand of the building, the indoor temperature is set constant at 21°C for both heating and cooling (Fig. 11). The ambient temperature is shown on the primary axis and the power demand on the secondary axis. The negative value in the secondary axis denotes a heating load, as TRNSYS uses a negative value for heating and positive value for cooling. There is a considerable delay of 17 hours in the power demand (red) when compared to the ambient temperature (blue) cycle, as shown in Fig. 11. An attenuation check is not possible in this case, due to the difference in the units.

In addition to the delay and attenuation, it is noted that the indoor temperature and power demand plot takes around 24 to 48 hours to stabilize. In other words, the mean value of the property takes about 24-48 hours to attain a constant value, i.e, due to the transient nature of the simulation, considerable time is required to stabilize the outputs. Henceforth, to illustrate the stabilization of indoor properties to a constant sinusoidal curve, the simulation is carried out for a period of 180 hours.

The property of thermal mass and thermal resistance influences the building envelope walls to mitigate the incident heat by absorbing and emitting the energy. Thus, by observing the delay and attenuation in this sensitivity study on indoor parameters, the effect of building envelope is conspicuous. On exhibiting this thermal behavior of the building envelope, the TRNSYS model is verified as reliable for further calculations.

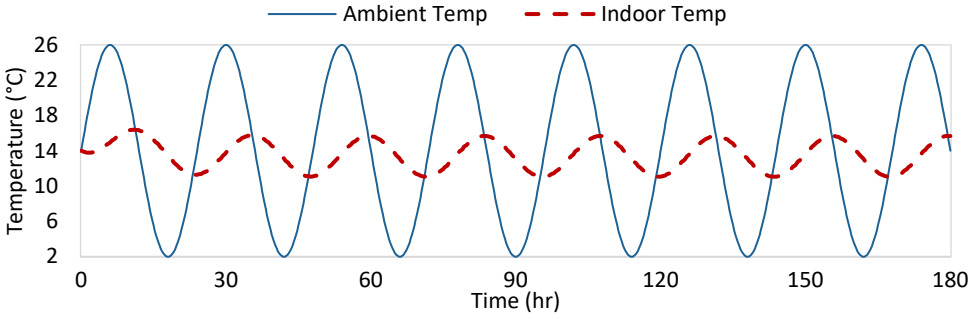

Fig 10. Variation of indoor temperature with time.

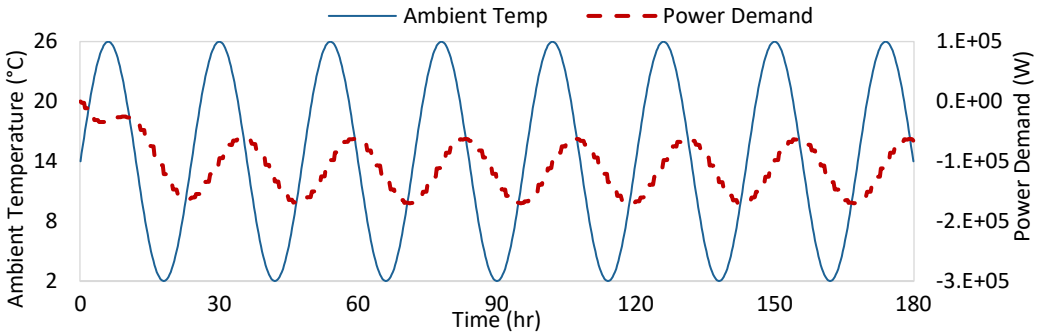

Fig 11. Variation of indoor power demand with time.

3.2 Predictive modeling

By examining the details of the reference building from Reddy et al. 2006 [29], the current work concentrates on the daily energy consumption (in kWh/day) averaged for a month. The objective is to model the energy consumption for each month of the year 2004 by inputting the required data into TRNSYS. The simulation's time step is one hour, which matches the frequency of the ambient weather data obtained from NSRDB. The direct output values from TRNSYS are given in power demand terms (kJ/hr), which are attained for every hour throughout the simulation. These values are averaged for one day and the values are converted to kW units (divide by 3600). The values for each day are summed for the complete month to give the total energy consumption (kW) for that particular period. Finally, the total energy consumption is multiplied by 24 hours and divided by the number of days in the month to give the average daily energy consumption for the month (in kWh/day),

$$Average\ daily\ energy\ consumption\ for\ the\ month\ = \frac{(P_1+P_2+P_3+\cdots+P_{Tmon})\times 24}{T_{mon}}\ , \qquad (16)$$

where P_n is the average power demand for a 24-hour cycle for the n^{th} day (kW) and T_{mon} is the number of days in that particular month.

The total daily energy consumption data for each month is derived by combining the heating and cooling power demand values. Two different infiltration rates, namely 0.25 ACH and 0.85 ACH, are considered, which accounts for the variability of wind speeds throughout the year. The minimum and maximum values of the total air changes per hour (ACH) for the building, which include the ventilation rate, are determined to be 0.4 ACH and 1.0 ACH, respectively. These values are well within the range of ACH values obtained using the 2017 ASHRAE Fundamentals [43], as detailed in section 2.2.3.1. The simulated values for both ACH rates are provided for all twelve months and are depicted in Fig. 12. The power consumption curve for 1.0 ACH (red curve) is observed to be higher than the curve for 0.4 ACH for all the months, with an average difference of 5705 kWh/day. It is notable that the measured results fall within the range of power consumption values for the minimum and maximum ACH rates. Therefore, it can be inferred that the actual ACH rate of this office building lies between 0.4 ACH and 1.0 ACH for all the months. Furthermore, from Fig. 12, it is observed that the measured consumption values during winter months are closer to the modeled values for 0.4 ACH than the values for 1.0 ACH, despite greater wind speeds. As well, Fig. 12 shows that for a given ACH value, energy usage during winter is greater than during summer.

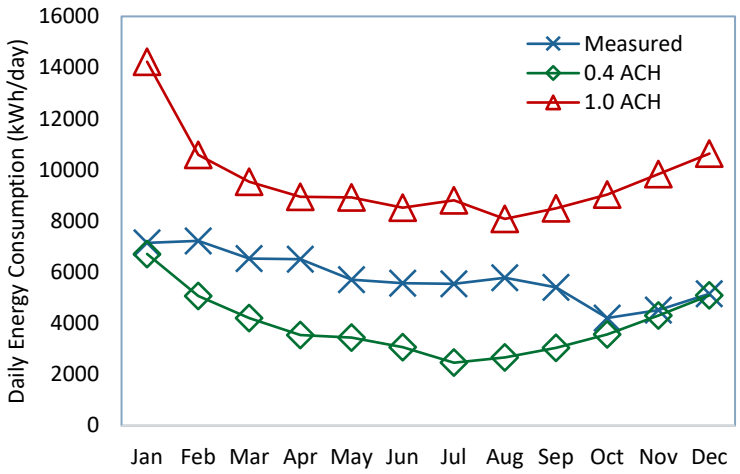

Fig 12. Building simulation plot for 0.4 ACH and 1.0 ACH.

4. Conclusion

Building managers, energy analysts, and policymakers may utilise predictive modeling of energy consumption in office buildings as a valuable tool to understand the trends of the building's energy usage, spot inefficiencies, and optimize energy usage. This work shows it is possible to develop predictive models that can forecast the energy consumption of a building with a high degree of accuracy by analysing historical data and other pertinent parameters such as ambient temperature, solar radiation, infiltration, ventilation, building envelope, internal lighting, equipment, occupancy, and ground temperature. To verify the reliability of the building model studied, an analysis is performed on indoor temperature and indoor power demand using sinusoidal weather data. The analysis reveals a dampened effect on indoor temperature (and indoor power demand) with a delay, attributable to the thermal mass and thermal resistance of the building envelope.

Some of the key parameters in predictive modeling (ambient temperature, solar radiation, and ground temperature) are varied hourly for two different ACH values, reflecting the unpredictability of the infiltration and ventilation rates. The results indicate that the measured energy consumption of the actual building falls between the curves of the two ACH rates: 0.4 ACH and 1.0 ACH. This suggests that the infiltration rates of the building, range from 0.25 ACH to 0.85 ACH, with a constant ventilation rate of 0.15 ACH. As well, the data presented illustrate that the energy consumption during winter is higher than during the summer, for the same ACH value. The analysis further reveals that a change of 0.6 ACH (= 1.0 - 0.4 ACH) corresponds to an annual average energy usage difference of 5705 kWh. The indoor ACH can be adjusted by altering the ventilation rate, regulating air flow from outside to inside of the building by opening and closing windows, and checking for cracks and leaks in the building's airtightness. These are important considerations when trying to reduce the energy usage of a building.

In addition to infiltration, other parameters also affect an office building’s energy consumption. To further improve the understanding of the factors affecting energy consumption in buildings, future work of this project will involve conducting a comprehensive sensitivity analysis of the building parameters. This analysis will provide insights into the relative importance of each parameter and how they contribute to energy consumption. By identifying the most influential parameters, engineers can prioritize their efforts towards reducing energy consumption by focusing on the parameters that have the greatest impact. Once the most influential parameters have been identified, appropriate strategies and methodologies can be proposed to mitigate energy usage. These might involve retrofits to the HVAC system or building envelope, adjustments to occupant routines or behaviour, or energy-saving technology. Engineers may significantly reduce energy use and related expenses while advancing sustainability objectives and lessening environmental impact by using a focused strategy to reducing energy usage.

Acknowledgements

This work is made possible by Natural Sciences and Engineering Research Council of Canada.

References

[1] K.H. Khan, C. Ryan, E. Abebe, Optimizing HVAC energy usage in industrial processes by scheduling based on weather data, IEEE Access 5 (2017) 11228-11235.

[2] D. Mariano-Hernández, L. Hernández-Callejo, A. Zorita-Lamadrid, O. Duque-Pérez, F. Santos García, A review of strategies for building energy management system: Model predictive control, demand side management, optimization, and fault detect & diagnosis, Journal of Building Engineering 33 (2021) 101692.

[3] Commercial Buildings Energy Consumption Survey (2018) CBECS final results [online] Available at: https://www.eia.gov/consumption/commercial/ (assessed on 2023-01-12)

[4] Microdata File, Commercial buildings energy consumption survey (CBECS), *US Department of Energy, Washington, DC, USA* (2015).

[5] NOAA Regional Climate Centers [online] Available at: www.rcc-acis.org (assessed on 2022-12-16).

[6] K. Papakostas, T. Mavromatis, N. Kyriakis, Impact of the ambient temperature rise on the energy consumption for heating and cooling in residential buildings of Greece, Renewable Energy 35 (2010) 1376–1379.

[7] H. Lia, K. Zhonga, J. Yua, Y. Kanga, Z.J. Zhaib, Solar energy absorption effect of buildings in hot summer and cold winter climate zone, China, Solar Energy 198 (2020) 519–528.

[8] S. Danov, J. Carbonell, J. Cipriano, J. Martí-Herrero, Approaches to evaluate building energy performance from daily consumption data considering dynamic and solar gain effects, Energy and Buildings 57 (2013) 110–118.

[9] Y. Huang and Y. Liu, Analysis on the influence of solar radiation on heating load of existing residential buildings in Western Sichuan, in IOP Conference Series: Materials Science and Engineering 556, no. 1 (2019) 012046.

[10] G. Hana, J. Srebricb, E. Enache-Pommer, Different modeling strategies of infiltration rates for an office building to improve accuracy of building energy simulations, Energy and Buildings 86 (2015) 288–295.

[11] S.J. Emmerich, A.K. Persily, Energy impacts of infiltration and ventilation in US office buildings using multizone airflow simulation, in: Proceedings of IAQ and Energy, Vol. 98, 1998, pp. 191–206.

[12] H. K. Dai, C. Chen, Air infiltration rates in residential units of a public housing estate in Hong Kong, Building and Environment 219 (2022) 109211.

[13] J. J. K. Jaakkola, P. Miettinen, Type of ventilation system in office buildings and sick building syndrome, American Journal of Epidemiology 141, no. 8 (1995) 755-765.

[14] American Society of Heating, Refrigerating and Air-Conditioning Engineers, ANSI/ASHRAE Standard 62.1, Standards for Ventilation for Acceptable Indoor Air Quality, New York, The Society, 2013.

[15] B.-L. Ahn, C.-Y. Jang, S. Leigh, S. Yoo, H. Jeong, Effect of LED lighting on the cooling and heating loads in office buildings, Applied Energy 113 (2014) 1484–1489.

[16] D. Jenkins and M. Newborough, An approach for estimating the carbon emissions associated with office lighting with a daylight contribution. Applied Energy 84 (2007) 608–622.

[17] Energy Information Administration. Commercial Buildings Energy Consumption Survey; 2003.

[18] Lighting standards and typical luminaires intended for office workplaces (2018) Understanding the Standards, but aiming higher [online] Available at: www.ledil.com/news_all/articles-and-whitepapers/office-lighting-standards/ (accessed on 2022-12-20).

[19] A.C. Menezes, A. Cripps, R.A. Buswell, J. Wright, D. Bouchlaghem, Estimating the energy consumption and power demand of small power equipment in office buildings, Energy and Buildings 75 (2014) 199–209.

[20] M. Badache, P. Eslami-Nejad, M. Ouzzane, Z. Aidoun, L. Lamarche, A new modeling approach for improved ground temperature profile determination, Renewable Energy 85 (2016) 436-444.

[21] S.W. Rees, Z. Zhou, H.R. Thomas, Ground heat transfer: A numerical simulation of a full-scale experiment, Building and Environment 42 (2007) 1478–1488.

[22] T. Kusuda and P.R. Achenbach, Earth temperature and thermal diffusivity at selected stations in the United States, National Bureau of Standards Gaithersburg MD, ASHRAE Transactions, Part 1 (1965) 71.

[23] A. Rasheed, C.S. Kwak, H.T. Kim, H.W. Lee, Building Energy an Simulation Model for Analyzing Energy Saving Options of Multi-Span Greenhouses. Applied Sciences 10, no. 19 (2020) 6884.

[24] D. Goodman, J. Chen, A. Razban, J. Li, Identification of Key Parameters Affecting Energy Consumption of an Air Handling Unit. In: *ASME International Mechanical Engineering Congress and Exposition*. American Society of Mechanical Engineers 50596 (2016) V06BT08A006.

[25] H. Zhao, F. Magoulès, A review on the prediction of building energy consumption, Renewable and Sustainable Energy Reviews 16 (2012) 3586– 3592.

[26] A. Stefanovic, D. Gordic, Modeling methodology of the heating energy consumption and the potential reductions due to thermal improvements of staggered block buildings, Energy and Buildings 125 (2016) 244–253.

[27] T.A. Reddy, I. Maor, C. Panjapornpon, Calibrating detailed building energy simulation programs with measured data—Part I: General methodology (RP-1051), HVAC&R Research 13, no. 2 (2007) 221-241.
[28] T.A. Reddy, I. Maor, C. Panjapornpon, Calibrating detailed building energy simulation programs with measured data—Part II: Application to three case study office buildings (RP-1051), HVAC&R Research 13, no. 2 (2007): 243-265.
[29] T.A. Reddy, I. Maor, C. Ponjapornpon, J. Sun, Procedures for reconciling computer-calculated results with measured energy data (RP-1051), Atlanta: American Society of Heating, Refrigerating and Air-Conditioning Engineers (2006).
[30] What is a Concrete Masonry Unit? (2016) Nitterhouse Masonry products [online] Available at: https://www.nitterhousemasonry.com/tips-advice/what-is-cmu/ (accessed on 2021-12-24).
[31] Ahmed Y Taha Al-Zubaydi, Building models design and Energy simulation with Google Sketchup and Openstudio, Journal of Advanced Science and Engineering Research 3, no. 4 (2013) 318-333.
[32] ASHRAE, 2017 ASHRAE Handbook: Fundamentals, 2017.
[33] S. E. G. Jayamaha, N. E. Wijeysundera, S. K. Chou, Measurement of the Heat Transfer Coefficient for Walls, Building and Environment, Vol. 31, no. 5 (1996) 399-407.
[34] E. M. Sparrow, J. W. Ramsey, E. A. Mass, Effect of finite width on heat transfer and fluid flow about an inclined rectangular plate, ASME Journal of Heat Transfer 101, (1979) 199-204.
[35] Wind speed data in Philadelphia (2014) Weather Underground [online] Available at: https://www.wunderground.com/forecast/us/pa/collegeville (accessed on 2022-12-05).
[36] A.S. Kalogirou, Solar Energy Engineering - Processes and Systems (2nd Edition), 2.3.8.1 Isotropic Sky Model, 2014, p.102.
[37] Engineering ToolBox (2009) Absorbed Solar Radiation. [online] Available at: https://www.engineeringtoolbox.com/solar-radiation-absorbed-materials-d_1568.html (accessed on 2022-12-12).
[38] C. P. Au-Yong, A. S. Ali, F. Ahmad, Improving occupants' satisfaction with effective maintenance management of HVAC system in office buildings, Automation in Construction 43 (2014) 31–37.
[39] M. Hadavi, H. Pasdarshahri, Quantifying impacts of wind speed and urban neighborhood layout on the infiltration rate of residential buildings, Sustainable Cities and Society 53 (2020) 101887.
[40] CIBSE. Chartered Institution of Building Services Engineers. CIBSE, 2021.
[41] D. S-K. Ting, Lecture Notes on Engineering Human Thermal Comfort, World Scientific, 2020, p.182.
[42] Hourly Weather Data in Philadelphia (1995) Annual Weather Averages [online] Available at: https://www.timeanddate.com/weather/usa/philadelphia/climate (accessed on 2021-12-10).
[43] American Society of Heating Refrigerating and Air-Conditioning Engineers, 2017 ASHRAE Handbook. Fundamentals, Atlanta GA, 2017.